https://doi.org/10.4047/jap.2025.17.6.380

Influence of misfit direction and abutment type on torque loss and fracture strength of implant-supported fixed dental prostheses

Vygandas Rutkūnas[1]*, Maisa Haiek[2], Daniel Kules[3], Liudas Auškalnis[1], Ieva Gendviliene[4], Ingrida Mischitz[5], Tan Fırat Eyüboğlu[6], Mutlu Özcan[7]

[1]Department of Prosthodontics, Institute of Odontology, Faculty of Medicine, Vilnius University, Vilnius, Lithuania
[2]Hadassah School of Dental Medicine, Hebrew University of Jerusalem, Jerusalem, Israel
[3]Department of Periodontology, Institute of Odontology, Faculty of Medicine, Vilnius University, Vilnius, Lithuania
[4]Department of Oral Surgery, Institute of Odontology, Faculty of Medicine, Vilnius University, Vilnius, Lithuania
[5]Department of Dental Medicine and Oral Health, Medical University of Graz, Graz, Austria
[6]Department of Endodontics, Faculty of Dentistry, Istanbul Medipol University, Istanbul, Türkiye
[7]Clinic of Masticatory Disorders and Dental Biomaterials, Center for Dental Medicine, University of Zurich, Zurich, Switzerland

ORCID
Vygandas Rutkūnas
https://orcid.org/0000-0001-5740-4573
Maisa Haiek
https://orcid.org/0009-0008-9970-4222
Daniel Kules
https://orcid.org/0000-0002-2897-3213
Liudas Auškalnis
https://orcid.org/0000-0001-6113-3753
Ieva Gendviliene
https://orcid.org/0000-0002-1777-9781
Ingrida Mischitz
https://orcid.org/0000-0002-3628-2922
Tan Fırat Eyüboğlu
https://orcid.org/0000-0002-0308-9579
Mutlu Özcan
https://orcid.org/0000-0002-9623-6098

Corresponding author
Vygandas Rutkunas
Department of Prosthodontics, Institute of Odontology, Faculty of Medicine, Vilnius University, Zalgirio str. 115, LT-08217 Vilnius, Lithuania
Tel +37068755661
E-mail vygandasr@gmail.com

Received August 25, 2025 / **Last Revision** November 20, 2025 / **Accepted** November 24, 2025

The study was supported by the Lithuanian Business Support Agency grant Nr. J05-LVPA-K-01-0055.

PURPOSE. This study aimed to evaluate the effects of fatigue and misfit on the reverse torque, load-bearing capacity, and failure modes of cemented and screw-retained two-implant-supported fixed dental prostheses (FDPs). **MATERIALS AND METHODS.** Eighty CAD-CAM zirconia frameworks with porcelain veneering were assigned to three groups based on engaging (E) and non-engaging (N) abutment configurations: N-N, N-E, and E-E. Misfit scenarios included a control cast and 100 μm horizontal or vertical misfits. Frameworks were mounted on implants as screw-retained or cement-retained 3-unit FDPs, forming seven test groups and one control group (n = 10). Reverse torque was measured before and after thermomechanical cycling, followed by maximum failure load (Fmax) testing and failure mode analysis. Fmax was evaluated using two-way ANOVA, and reverse torque using mixed-effects ANOVA accounting for engagement, misfit, and implant position (α = 0.05). **RESULTS.** No significant differences in Fmax were observed across zirconia specimen groups or engagement configurations under various misfit conditions ($P > .05$). Engagement configuration did not significantly impact fracture strength or reverse torque ($P = .421$). A significant difference was found in the horizontal misfit group compared to controls ($P < .001$). Reverse torque values differed between distal (13.5 ± 0.5 Ncm) and mesial implants (18.6 ± 0.5 Ncm) ($P = .000$), suggesting distal implants may be more prone to preload loss and mechanical issues. **CONCLUSION.** The engagement configuration of implants did not significantly affect reverse torque, fracture strength, or failure modes of cemented and screw-retained restorations, although horizontal misfit reduced load-bearing capacity. [J Adv Prosthodont 2025;17:380-91]

KEYWORDS
CAD-CAM; Dental implants; Dental materials; Implant-supported dental prosthesis; Prosthodontics

pISSN 2005-7806 • eISSN 2005-7814

INTRODUCTION

Implant therapy offers long-term success for missing teeth,[1-4] with a 96.4% survival rate after 5 years, 93.9% after 10 years,[2,3] and 93% after 20 years.[4] Mechanical complications—including screw loosening, framework misfit, and loss of preload—continue to pose significant concerns, potentially undermining the stability of the restoration.[5,6] The orientation and extent of prosthesis misfit are especially critical, as even minimal discrepancies can significantly influence stress distribution and long-term biomechanical performance.[7-9] Proper torque application and thermocycling conditions are recommended for studying implant components.[10,11] Screw-retained implant-supported fixed dental prostheses (FDP) offer rigidity and retrievability, while cement-retained restorations simplify procedures and compensate better for the misfit due to the cement gap but at the same time increase the risk of inflammation and implant failure.[12,13]

Combining screw-retained frameworks with engaging and non-engaging abutments maximizes load distribution, improves prosthesis fit, and reduces stress concentration.[14-16] Engaging and non-engaging abutments represent two key options for connecting prostheses to implants.[14-18] Engaging abutments feature an anti-rotational design, such as a hex or star-shaped interface, that locks the abutment into the implant and prevents rotation, which is advantageous for single-unit restorations requiring precise orientation.[14-17] Non-engaging abutments, by contrast, allow rotational freedom and facilitate passive fit in multi-unit FDPs, accommodating slight implant angulation discrepancies and reducing stress concentrations.[15-18] Combinations of engaging and non-engaging abutments can optimize prosthesis stability, load distribution, and fit, balancing the need for anti-rotation with the flexibility to minimize mechanical complications.[17-19]

Biomechanical principles significantly influence implant-retained restorative operations, impacting parameters such as prosthesis fit, masticatory pressures, implant position, component materials, and implant success.[20-22] Passive fit, with a maximum misfit of 150 μm, is generally acceptable.[23] Misfits can cause biomechanical issues, late implant failure,[24] and mechanical complications.[25-27]

Human errors and fabrication faults significantly affect the fit of implant-borne FDPs.[28] Digital technology replaces traditional workflows,[29] but still introduces errors and inaccuracies, leading to misfit and treatment failure.[16,28] In this context, using a 100 μm misfit threshold in experimental studies has been justified as it represents a clinically meaningful magnitude for both vertical and horizontal orientations.[9] The literature on implant-supported restorations is inconclusive, and studies are needed to optimize clinical success.

To the authors' best knowledge, few studies[16,28,29] have compared different misfit scenarios and torque changes as a function of various configurations of implant-supported screw-retained FDPs using multiple engaging and non-engaging Ti-base configurations. Yet, these were performed independently without considering these parameters in a combined study design. Therefore, this study's objectives were[1] to evaluate the mechanical properties of screw-retained and cement-retained restorations with different combinations of abutments (non-engaging / non-engaging (N-N group), engaging / non-engaging (N-E group), and engaging / engaging (E-E group)) under simulated horizontal and vertical misfits in fatigue conditions;[2] to measure the reverse torque before and after aging conditions and determine the effects of fatigue and implant location on the retention of screw preload.

MATERIALS AND METHODS

A pilot study (n = 5) was conducted to determine the sample size, considering the following parameters: α = 0.05, d = 0.848, and *P* = .95. ANOVA, fixed effects, omnibus, and one-way tests were applied. The effect size (d = 0.848) was derived from the pilot study and represented a large effect according to Cohen's classification, reflecting the expected magnitude of group differences under misfit conditions. Power analysis was performed using G*Power statistical software (ver. 3.1.9.7; Heinrich-Heine-Universität, Düsseldorf, Germany), which resulted in a computed sample size of 9. In order to account for nonparametric statistical

https://doi.org/10.4047/jap.2025.17.6.380

analysis, the sample size was increased to 10 specimens for each group.

Experimental models were created to simulate a mandibular second premolar to the second molar FDP (fixed partial denture) restoration. This was achieved by placing two implants (Ø4.3 × 13 mm, 7.5° internal connection, Conelog Screw-Line; Camlog Biotechnologies AG, Basel, Switzerland) with a span of 22 mm between the centers of the top plane of the implants in the Frasaco model (Frasaco GmbH, Tettnang, Germany). The implants were set at an angle of 10° relative to each other, replicating the clinical scenario.[30]

In this study, scan bodies (ConelogScanbody, Ø 3.8 / Ø 4.3) were attached to the two implants and scanned using an intraoral scanner (Trios 4, 3ShapeA/S, Copenhagen, Denmark) to capture the digital impressions. Full-contour 3-mol% yttria stabilized zirconia (ZrO_2 FDPs (Noritake Katana HTML Plus; Kuraray Noritake Dental Inc., Tokyo, Japan) were fabricated according to the manufacturer's recommendations using a digital workflow in a standardized procedure. The mesial connector height was 4.9 mm with a width of 3.6 mm (14.8 mm^2), while for the distal connector, the height was 6.6 mm, and the width was 4.7 mm (18.8 mm^2). The FDPs consisted of a zirconia framework buccally veneered with feldspathic porcelain (1 mm thickness) (Cerabien ZR; Kuraray Noritake Dental Inc., Tokyo, Japan).

The frameworks (N = 80) were divided into three groups using the True Random Number generator (Random.org; Mads Haahr, Dublin, Ireland) based on the attached Ti-base combinations (Ø4.3 × 2 mm, Conelog; Camlog Biotechnologies AG, Basel, Switzerlan): N-N type: two non-engaging Ti-bases on mesial (M) and distal (D); a semi-engaging type N-E group: one non-engaging Ti-base on side M and one engaging Ti-base on side D; and for the engaging type E-E: two engaging Ti-bases on sides M and D. Screw-retained prostheses were fabricated for the N-N and N-E specimens, and cement-retained ones for the E-E specimens.

Each group was further categorized based on the engagement configuration and misfit simulation level:

1. Screw-retained N-N restorations (0 misfit - control group)
2. Screw-retained N-N restorations (100 micron vertical misfit)
3. Screw-retained N-N restorations (100 micron horizontal misfit)
4. Screw-retained N-E restorations (0 misfit - control group)
5. Screw-retained N-E restorations (100 micron vertical misfit)
6. Screw-retained N-E restorations (100 micron horizontal misfit)
7. Cement-retained E-E restorations (0 misfit - control group)
8. Cement-retained E-E restorations (100 vertical misfit).

In the cement-retained (E-E) groups, custom zirconia abutments (Noritake, Katana HTML Plus) 5.5 mm in height and 3 degrees taper were fabricated and cemented on engaging Ti-bases.

A reference cast was created to ensure consistent cementation. A "zero" framework was selected and cemented (Panavia V5; Kuraray Noritake Dental Inc., Tokyo, Japan) to two engaging Ti-bases under microscopic vision (Mobiliskope S; Renfert GmbH, Hilzingen, Germany) to ensure optimal fit and complete seating. Cementation was performed after air-abrasion of the intaglio surfaces and the abutments with 50-micron Al_2O_3 at a pressure of 0.2 MPa from a distance of 10 mm for 15 seconds, followed by primer application (Clearfil Ceramic Primer Plus; Kuraray Noritake Dental Inc., Tokyo, Japan). The FDPs with incorporated Ti-bases were then attached to mock implants (Conelog Screw-Line; Camlog Biotechnologies AG, Basel, Switzerland) and secured at 20 Ncm. Type IV dental stone (GC FUJIROCK EP; GC Corporation, Tokyo, Japan) was poured around the implants, forming the reference cast. Then, all screw-retained FDPs and custom zirconia abutments were cemented (Panavia V5; Kuraray Noritake Dental Inc., Tokyo, Japan) onto the Ti-bases using the same reference cast as a guide to achieve consistency. Polishing and cleaning protocols were performed following the cement manufacturer's recommendations (Fig. 1).

To create simulated misfit scenarios, three definitive casts (GC FUJIROCK EP; GC Corporation, Tokyo, Japan) were generated with different fits: a control

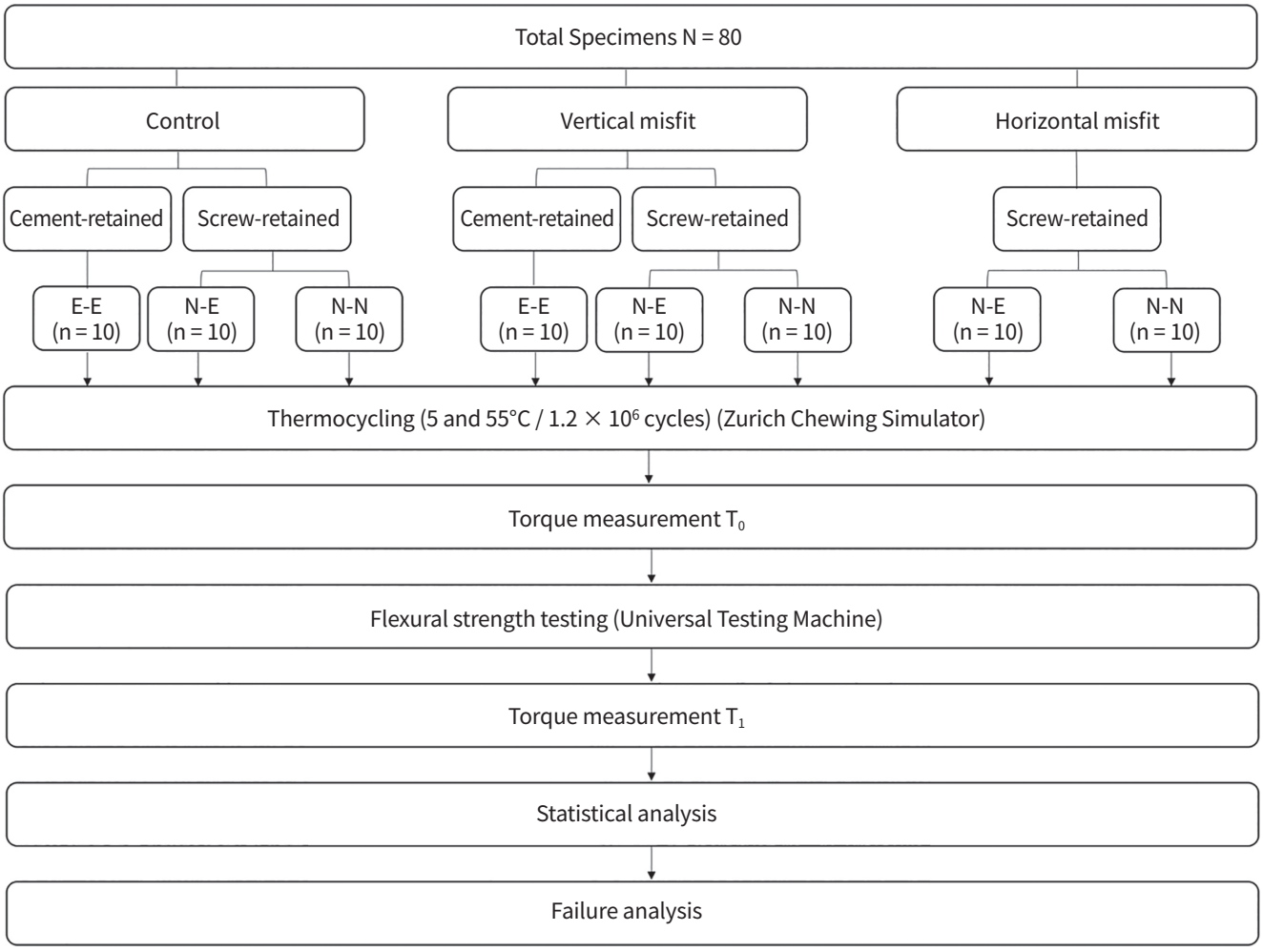

Fig. 1. Experimental workflow and specimen distribution.

cast with no misfit (0 μm), a cast with horizontal misfit (100 μm), and a cast with vertical misfit (100 μm). The implant positioning for simulation of the different fits in the casts was achieved using a micromechanical stand as described in previous studies.[16,28] After creating the horizontal or vertical misfit on the stand, two open-tray impression copings were connected and splinted with auto-polymerized resin (Pattern resin, GC America Inc., Alsip, IL, USA). After the resin was set, the copings were removed, and two real implants (Conelog Screw Line, 4.3 × 13) were connected. Then, a type IV dental stone (GC FUJIROCK EP; GC Corporation, Tokyo, Japan) was poured to secure the implants, create the test models, and simulate different misfit levels.

The finalized FDPs were cleaned using steam and fitted onto the implants embedded into the dedicated test and control models. The screw-retained FDPs were seated onto their respective models, and the screws were tightened to 20 Ncm using a mechanical torque device.

For the cement-retained FDPs (n = 20), the intaglio surfaces of the prosthesis were pretreated using air-abrasion with 50 μm Al_2O_3 particles at a pressure of 0.2 MPa from a distance of 10 mm for 15 seconds. Following this, the prostheses were cleaned in an ultrasonic bath with 96% ethanol for 5 minutes and then air-dried for 15 seconds. A phosphate-containing primer (Clearfil Ceramic Primer Plus; Kuraray Noritake Dental Inc., Tokyo, Japan) was applied to the fitting surface using a brush-on application technique. A thin, uniform layer of adhesive resin cement (Panavia

https://doi.org/10.4047/jap.2025.17.6.380

V5; Kuraray Noritake Dental Inc., Tokyo, Japan) was then spread. Thereafter, the framework was gently seated over the ZrO_2 abutments on the designated casts for the control and test groups. Excess cement was carefully removed, and the cement was photo-polymerized using a photo-polymerization unit (light output: 600 mW/cm^2, Optilux 501; Kerr Corporation, Orange, CA, USA) at a distance of 5 mm from each site for a total of 40 seconds, following the manufacturer's instructions. This procedure was consistently repeated for all frameworks in this group, and one operator conducted all placements (Fig. 2).

Specimens were subjected to thermocycling and mechanical loading between 5°C and 55°C for 1.2 × 10^6 cycles of dynamic loading with a dwell time of 120 s at each temperature and a fluid exchange time of 10 s. The dynamic loading was performed using a 49 N load at a frequency of 1.67 Hz in a computer-controlled cyclic loading machine (Zurich Chewing Simulator) with a Ø5/8-inch crosshead descending perpendicularly at a speed of 30 mm/s on the central point of the occlusal surface of the pontic. The load magnitude (49 N) and frequency (1.67 Hz) were chosen to simulate physiologic masticatory forces *in vitro*, consistent with previous studies reporting that chewing forces in fatigue simulations typically range from 40 – 50 N.[10,11] At an estimated average of 250,000 – 300,000 chewing cycles per year,[31] the applied 1.2 × 10^6 cycles approximate 4 – 5 years of clinical function, thereby providing a rigorous aging protocol for the tested specimens. Reverse torque values were measured using a Mark-10 M7i professional digital force/torque indicator (TEquipment, Long Branch, NJ, USA) at two time points: immediately after thermomechanical loading cycles (T_0) and after fatigue testing on identical specimens (T_1) (Fig. 3). A new set of screws was used for T_1 measurements to avoid confounding effects from screw deformation or prior loosening,

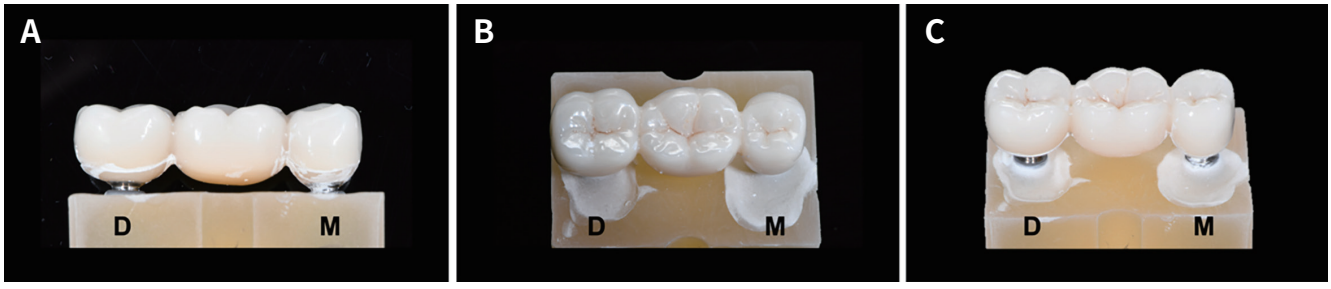

Fig. 2. Experimental model preparation. (A) Overview of the cemented FDP on mesial (M) and distal (D) implants with engaging abutments in the 100-μm vertical misfit simulation. (B) Close-up view of the mesial (M) abutment. (C) Close-up view of the distal (D) abutment.

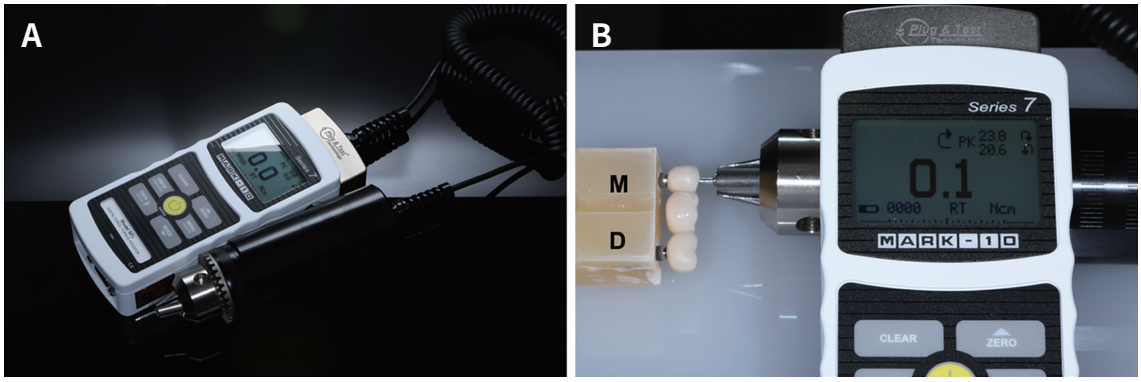

Fig. 3. Reverse torque measurement in a screw-retained implant bridge using a Mark-10 M7i professional digital force/torque indicator (TEquipment, Long Branch, NJ, USA) (A). The torque values recorded for the mesial implant (M) in the screw-retained implant bridge are depicted (B).

ensuring that the removal torque reflected the effect of fatigue and misfit rather than repeated use of the same screws. To evaluate the impact of thermomechanical cyclic loading, the mean reverse torque values of the two screws in each specimen were determined, and the delta change was calculated relative to the initial end torque values. Reverse torque values of mesial and distal implants were evaluated separately to investigate whether implant position contributes to preload loss. Implant position is a known factor influencing torque due to occlusal loading patterns, as supported in prior literature.[32]

Surviving specimens were loaded in a universal testing machine (Z010; ZwickRoell GmbH & Co. KG, Ulm, Germany) at a crosshead speed of 1 mm/min. An experienced prosthodontist used a digital microscope (Digital Microscope VHX-2000; Keyence Corporation, Osaka, Japan) at 40× magnification to examine all specimens and evaluate the failure modes. The failure modes were classified based on fracture type and location: transversally at the distal connector area, fossa to mesial connector, fossa to distal connector, both connectors, distal connector, failure (no recorded max force).

The failures were analyzed using a digital microscope (VHX-200; Keyence Corporation, Osaka, Japan) at different magnifications to examine screw deformation and the Ti-Base implant-interface seal.

All data were first tested for normality and homogeneity of variances using the Kolmogorov-Smirnov test. For maximum load (Fmax), a two-way ANOVA was performed with 'abutment engagement' and 'misfit type' as factors, followed by Tukey's post hoc test. Reverse torque values were analyzed using a mixed-model ANOVA, with 'implant position' (mesial vs. distal) as an additional factor. The significance level was set at $\alpha = 0.05$ (IBM SPSS Statistics for Windows, v26; IBM Corp., Armonk, NY, USA).

RESULTS

All specimens withstood fatigue conditions without any fractures, except for one screw-retained specimen with a vertical mismatch, notably in a non-engaged-engaged configuration, where a broken screw was encountered. The mean and standard deviation of all misfit groups (control = 0 µm, H = 100 µm, V = 100 µm) are presented in Table 1, including 95% confidence intervals to highlight variability and differences among the groups.

All specimens withstood fatigue conditions without any fractures, except for one screw-retained specimen with a vertical mismatch in the non-engaged–engaged configuration, where a broken screw was observed. The statistical analyses showed no significant effect of abutment engagement ($F = 1.12$, $P = .294$) and no engagement × misfit interaction ($F = 0.92$, $P = .421$) on fracture strength. Only the misfit factor itself was significant ($F = 6.37$, $P < .001$), driven by the horizontal misfit groups, which fractured at lower

Table 1. Mean (± SD) values with 95% confidence intervals (CI) of maximum load to fracture (Fmax, N) for different engagement configurations and misfit conditions

Misfit group	Engagement system	Sample size (n)	Fmax (N) Mean ± SD	95% CI Lower	95% CI Upper
Control	NN	10	1828.06 ± 473.63	1534.50	2121.62
	NE	10	1758.70 ± 255.76	1600.18	1917.22
	EE	10	1284.54 ± 283.71	1108.69	1460.39
Vertical	NN	10	2119.74 ± 453.71	1838.53	2400.95
	NE	9*	1816.18 ± 327.39	1602.29	2030.07
	EE	10	1563.26 ± 404.36	1312.64	1813.88
Horizontal	NN	10	1509.20 ± 179.64	1397.86	1620.54
	NE	10	1557.25 ± 283.67	1381.43	1733.07

The groups included control (C = 0 µm), horizontal misfit (H = 100 µm), and vertical misfit (V = 100 µm).
The asterisk (*) indicates a lost specimen due to a broken screw. NN: non-engaged – non-engaged; NE: non-engaged – engaged; EE: engaged – engaged.

https://doi.org/10.4047/jap.2025.17.6.380

loads than the control ($P < .001$). Vertical misfit did not differ from control ($P > .05$). Mixed-model ANOVA for reverse torque revealed a significant implant-position effect (mesial > distal; $P < .001$) but no effect of engagement configuration ($P = .318$) or misfit ($P = .267$), and no significant interactions (all $P > .05$). Occasional T_1 values exceeded T_0 (e.g., Control NN mesial), reflecting friction and new screws at T_1 rather than a true preload increase, supported by overlapping CIs and nonsignificant ANOVA results (Table 2).

The failure-mode analysis (shown in Table 3) revealed that cracks most often started at the point where the pontic and distal connector meet. This was true regardless of how the abutment was engaged. Additionally, a greater horizontal misfit seemed to lead to more fractures at the distal connector (Figures 4 and 5). Transversal fractures at the distal connector were mainly seen in NN control and vertical misfit groups. In contrast, fossa-to-distal connector fractures were common in NE and EE groups, especially under horizontal misfit. Failures involving both connectors or isolated distal fractures were rare; only one early failure (broken screw) occurred in NE vertical misfit. Cross-sectional microscopic analysis further demonstrated the implant-abutment connection, with the fixation screw in place.

Table 2. Reverse torque measurements of screw-retained implant restorations

Misfit group	Engagement system	Sample size (n)	Implant position	T_0 Mean ± SD	T_0 95% CI	T_1 Mean ± SD	T_1 95% CI
Control	NN	4	M	21.325 ± 2.246	17.751 – 24.899	25.700 ± 2.246	22.126 – 29.274
Control	NN	4	D	21.750 ± 2.246	18.176 – 25.324	14.700 ± 2.246	11.126 – 18.274
Vertical	NN	6	M	14.050 ± 1.834	12.125 – 15.975	13.233 ± 1.834	11.308 – 15.158
Vertical	NN	6	D	14.483 ± 1.834	12.558 – 16.408	12.400 ± 1.834	10.475 – 14.325
Horizontal	NN	6	M	13.867 ± 1.834	11.942 – 15.792	14.450 ± 1.834	12.525 – 16.375
Horizontal	NN	6	D	13.983 ± 1.834	12.058 – 15.908	11.900 v 1.834	9.975 – 13.825
Control	NE	10	M	16.670 ± 1.420	15.654 – 17.686	14.980 ± 1.420	13.964 – 15.996
Control	NE	10	D	9.070 ± 1.420	8.054 – 10.086	10.730 ± 1.420	9.714 – 11.746
Vertical	NE	10	M	21.873 ± 1.354	20.904 – 22.842	23.109 ± 1.354	22.140 – 24.078
Vertical	NE	10	D	10.755 ± 1.354	9.786 – 11.724	17.345 ± 1.354	16.376 – 18.314
Horizontal	NE	10	M	20.130 ± 1.420	19.114 – 21.146	24.770 ± 1.420	23.754 – 25.786
Horizontal	NE	10	D	10.890 ± 1.420	9.874 – 11.906	14.630 ± 1.420	13.614 – 15.646

The means, standard deviations, and 95% confidence intervals of initial torque values (T_0) and end torque values (T_1) were recorded before and after thermocycling and mechanical loading for different engagement systems on both mesial (M) and distal (D) implants.
Data are presented for all misfit groups (Control = 0 µm, Horizontal = 100 µm, and Vertical = 100 µm). NN: non-engaged – non-engaged; NE: non-engaged – engaged.

Table 3. Summary of fracture types and location based on misfit levels

Failure type and location	V (N-N)	V (N-E)	V (E-E)	C (N-N)	C (N-E)	C (E-E)	H (N-N)	H (N-E)
Transversally at the distal connector area	4	0	0	6	0	0	4	0
Fossa to mesial connector	5	5	0	3	3	5	4	3
Fossa to distal connector	1	4	8	1	6	5	2	7
Both connectors	0	1	1	0	1	0	0	0
Distal connector	1	0	1	1	0	1	0	0
Failure (no recorded max force)	0	1	0	0	0	0	0	0

(Control = 0 µm, Horizontal = 100 µm, and Vertical = 100 µm. NN: non-engaged – non-engaged, NE: non-engaged – engaged.)

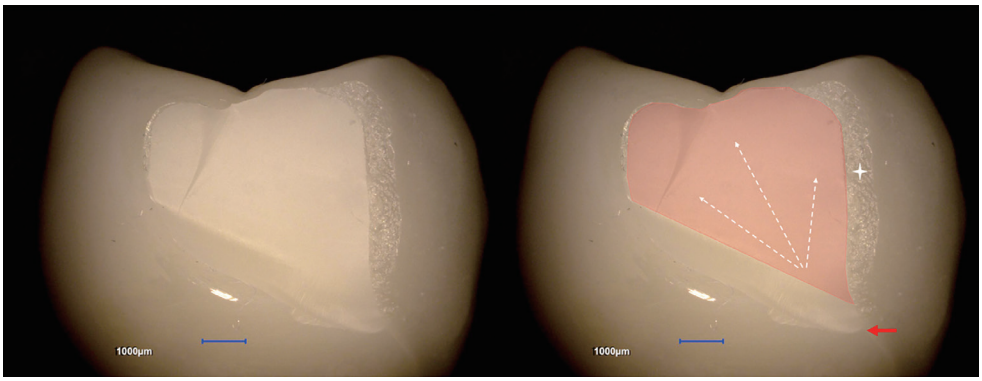

Fig. 4. Different failure modes and locations of the various engagement configurations.

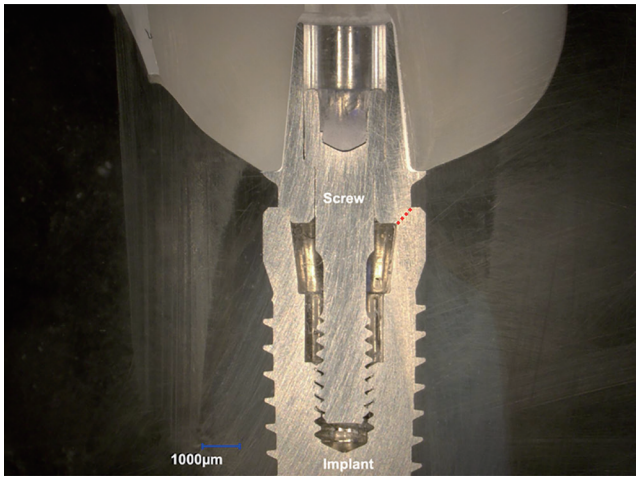

Fig. 5. Cross-sectional microscopic view of an implant-abutment assembly. The zirconia abutment, fixation screw, and titanium implant are shown in section. The red dotted line marks the abutment-implant interface area.

DISCUSSION

This study examined the effects of implant engagement style, 100 μm misfit orientation (horizontal or vertical), and implant position on the fracture strength and removability of zirconia three-unit FDPs. Results showed that engagement style had no significant effect on fracture strength or torque loss, and importantly, no significant interaction was found between engagement and misfit, suggesting that the impact of misfit on restoration performance occurs independently of the engagement configuration. Misfit orientation, however, had a significant influence on fracture strength, with horizontal misfits resulting in lower Fmax compared to the control, while vertical misfits did not differ from the control. The null hypothesis was therefore rejected for misfit orientation and implant position, while engagement configuration and the engagement and misfit interaction were not significant. These findings highlight the critical role of horizontal misfit in restoration integrity, supporting prior studies that emphasized misfit orientation as a determinant of mechanical behavior.[13,23,33] Engagement configuration did not significantly modify the effect of misfit, indicating that reducing misfit alone, rather than altering engagement type, may be more important for enhancing mechanical performance. The lack of significant difference related to abutment type is mainly due to zirconia frameworks' high rigidity. This rigidity likely hid subtle differences between engaging and non-engaging connections, as zirconia's strength and stiffness mainly affect load transfer. As a result, the connection geometry's effect on fracture resistance and torque may be minimal. Using standardized connector sizes and a uniform CAD-CAM process could also have unified stress distribution among groups, reducing observable effects of abutment type. This aligns with previous studies showing that material properties and rigidity can overshadow connection-specific effects.[16,28,29]

The study replicated cyclic loading forces during mastication and aging on dental materials using thermomechanical cycling.[11] Although the 49 N cyclic load is within documented chewing forces, it represents the lower end of normal mastication. Typi-

https://doi.org/10.4047/jap.2025.17.6.380

cal chewing forces range from 10 to 120 N, depending on the type of food and individual differences,[2-6] with higher forces between 190 and 360 N occurring only during maximal biting rather than normal mastication.[7-10] This load offers a conservative simulation; however, higher functional or parafunctional loads can increase stress and the risk of mechanical issues at the prosthesis and implant interface.[31] Consequently, the protocol may underestimate the stresses experienced under heavier loads or bruxism conditions. Most specimens remained intact, showing restoration stability, but one broken screw indicates vulnerabilities, requiring larger samples and clinical research. Cyclic loading and misfit type did not significantly affect reverse torque across engagement configurations; however, implant position did, with distal implants exhibiting significantly greater torque loss than mesial implants. This contrasts with prior findings that non-engaging setups tolerate misfit.[28] Alzoubi *et al*.[29] also saw no significant preload difference among abutment configurations, suggesting standardization may not enhance outcomes but could streamline procedures.

Compared to a non-engaging (NN) design, a NE abutment configuration is expected to improve implant-to-abutment stability and reduce screw loosening.[17,32,34] Data confirms a significant difference in reverse torque between distal and mesial implants, with the distal showing more pre-load loss. It is important to note that, in some instances, T_1 values exceeded T_0 (e.g., Control NN mesial). This outcome reflects the influence of interface friction rather than preload. Embedment/settling and the use of new screws at T_1 can increase friction and yield higher loosening torque, although overlapping CIs and ANOVA results confirmed that these changes were not statistically significant.[32,33] Factors like applied torque, screw design,[29] implant position, biomechanical forces,[34] load distribution, and tightening sequence may cause torque variation.[16,28] The greater torque loss in distal implants suggests higher susceptibility to stress and long-term issues. These variations highlight the need to consider implant position and associated mechanical stress complications.

The implant-abutment contact area is crucial for stress distribution. Bone-level implants have a smaller contact area near the crestal bone, increasing stress concentration and risking peri-implant bone loss.[35,36] Tissue-level implants have a wider, more coronally placed contact area, distributing forces more evenly and reducing stress on the marginal bone.[36,37] However, this may transfer more load to the abutment and screw, affecting stability.[36] These differences suggest implant design should consider both biological and mechanical factors for long-term success.

The choice between cement- and screw-retained dental implant restorations is unclear. A systematic review found that cemented restorations caused more bone loss.[38] Conversely, Nissan *et al*. reported better long-term results with cement-retained crowns.[39] When evidence conflicts, factors may favor screw-retained options. Cemented prostheses are hard to remove, so screw retention is preferred for extensive cases needing regular care. Achieving a passive fit with screw-retained prostheses is challenging. Cement layers can act as stress absorbers, making cement-retained structures more passive, but distortions can occur in any laboratory or clinical step. Advances in manufacturing now allow screw-retained restorations to fit precisely, reducing screw loosening.[40]

Although this study did not directly compare cemented and screw-retained prostheses, it is important to interpret our results within the larger context of existing scientific research. A comprehensive systematic review conducted by Heckmann *et al*. showed that cemented restorations tend to have more peri-implant bone loss compared to screw-retained options.[35] Conversely, a long-term clinical study by Nissan *et al*. found high survival rates for cement-retained crowns, demonstrating their clinical usefulness.[39] These different findings highlight the need to distinguish between biological complications and the longevity of the prosthesis. It is crucial for clinicians to carefully consider both mechanical and biological factors when choosing the most suitable type of restoration, as this decision affects not only short-term results but also the long-term success of the implant.

Fracture analysis reveals failure patterns in FDPs, highlighting how tensile stresses cause crack initiation and propagation, mainly in the occlusal direc-

tion. A detailed analysis of failure patterns across misfit levels and Ti-base combinations shows distinct trends. Transverse failures at the distal connector were mostly seen in the control and vertical misfit groups with N-N combinations, indicating the distal connector as a critical stress point under these conditions. No such failures were noted in N-E and E-E setups, hinting at the influence of engaging interfaces on stress distribution. Failures from the fossa to the mesial connector were common across all groups, especially in the E-E control and N-N and N-E vertical misfits, due to stress at the pontic-connector interface. Fractures from the fossa to the distal connector were the most frequent in E-E and N-E groups, revealing their vulnerability to tensile stress, with some failures linked to horizontal misalignment. Few failures involved both connectors or only the distal connector, and a single early failure was seen in the V group. These results emphasize how misfit level and Ti engagement affect FDP fracture behavior. The absence of certain failure modes in E-E setups, particularly transversal fractures at the distal connector, suggests better load distribution, warranting further study. These findings highlight the importance of connector design. Increasing its cross-sectional area, especially at the distal end, reduces tensile stress and fracture risk in screw-retained FDPs. Optimizing connector height and width is advisable when expecting horizontal misfit, while minimizing sharp internal angles can improve stress distribution. Such design tweaks could turn lab results into practical ways to boost prosthesis durability. The higher distal connector failure rate in V and C groups highlights the need to optimize connector design to minimize tensile stress. These findings contrast with previous research showing internal connections with materials like titanium or zirconia having higher fracture strength after cyclic loading. The behavior of the engaging types (N-E and E-E) may provide insights into stress distribution, but further research is needed to evaluate the benefits of internal connections for stress management and durability.

In the present study, force transmission predominantly occurred via direct contact at the implant platform. The non-engaging segment of the abutment was designed so that it did not make contact with the implant, thereby ensuring optimal alignment and stability. This configuration facilitated a more passive fit, which is crucial for maintaining implant integrity and function.

This study only tested one type of zirconia and implant, which limits how broadly the results can be applied. The misfit scenarios were limited to horizontal and vertical misfits at 100 µm, which might not capture the full range of clinical situations where misfits could be larger. Additionally, using just one zirconia material and a single implant system could have hidden potential differences in torque stability and fracture resistance that depend on specific materials or systems. Furthermore, the cyclic load of 49 N applied here aligns with the lower range of normal chewing forces, which may not fully represent the occlusal loads experienced in clinical settings. While this load was selected to standardize fatigue tests and avoid early failures, the relatively low force could limit how broadly the fatigue results can be applied. Future research should consider different zirconia generations, veneering protocols, or implant–abutment designs, as these could lead to different results. Clinical studies should report the parameters and outcomes studied here to validate findings. Without these reports, systematic reviews and clinical trials cannot provide guidelines for implant-borne FDPs. Unlike previous research[16,28,29] that examined engagement or misfit in isolation, this study integrated both factors within a factorial design, enabling exploration of interaction effects and offering a more clinically relevant interpretation. Including torque retention, engagement type, and simulated misfits under fatigue loading provides a comprehensive biomechanical profile. Future research should explore wider misfit magnitudes, materials, and implant systems to validate and expand findings. Longer-term clinical trials are necessary to assess the effects of misfit on the survival, stability, and biological implications of restorations.

CONCLUSION

From this study it could be concluded that the engagement configurations did not significantly affect the fracture strength of screw- or cement-retained

implant-borne FDPs under simulated misfit scenarios after fatigue conditions. Distal implants exhibited greater torque loss than mesial implants, highlighting implant position as a clinically relevant factor for prosthesis stability. Although horizontal and vertical misfits up to 100 μm did not compromise removal torque, horizontal misfits were associated with more unfavorable fracture patterns at the distal connector. Horizontal misfit was identified as the critical factor reducing fracture strength, underscoring the importance of optimizing connector design and minimizing misfit levels to enhance the structural integrity and long-term performance of FDPs.

ACKNOWLEDGMENTS

The materials were kindly donated by Kuraray Noritake and Oral Reconstructive Foundation.

REFERENCES

1. Duong HY, Roccuzzo A, Stähli A, Salvi GE, Lang NP, Sculean A. Oral health-related quality of life of patients rehabilitated with fixed and removable implant-supported dental prostheses. Periodontol 2000 2022;88:201-37.
2. Pjetursson BE, Thoma D, Jung R, Zwahlen M, Zembic A. A systematic review of the survival and complication rates of implant-supported fixed dental prostheses (FDPs) after a mean observation period of at least 5 years. Clin Oral Implants Res 2012;23 Suppl 6:22-38.
3. Moraschini V, Poubel LA, Ferreira VF, Barboza Edos S. Evaluation of survival and success rates of dental implants reported in longitudinal studies with a follow-up period of at least 10 years: a systematic review. Int J Oral Maxillofac Surg 2015;44:377-88.
4. Roccuzzo A, Imber JC, Marruganti C, Salvi GE, Ramieri G, Roccuzzo M. Clinical outcomes of dental implants in patients with and without history of periodontitis: a 20-year prospective study. J Clin Periodontol 2022;49:1346-56.
5. Sahin S, Cehreli MC. The significance of passive framework fit in implant prosthodontics: current status. Implant Dent 2001;10:85-92.
6. Abduo J, Judge RB. Implications of implant framework misfit: a systematic review of biomechanical sequelae. Int J Oral Maxillofac Implants 2014;29:608-21.
7. Spazzin AO, Dos Santos MB, Sobrinho LC, Consani RL, Mesquita MF. Effects of horizontal misfit and bar framework material on the stress distribution of an overdenture-retaining bar system: a 3D finite element analysis. J Prosthodont 2011;20:517-22.
8. Caldas RA, Pfeifer CSC, Bacchi A, Santos MBFD, Reginato VF, Consani RLX. Implant inclination and horizontal misfit in metallic bar framework of overdentures: analysis by 3D-FEA method. Braz Dent J 2018;29:166-72.
9. Arshad M, Asgari A, Kharazifard MJ, Ameri N. Effect of implant angulation on the rotational displacement of a 3-unit bridge after digital impression. Int J Dent 2022;2022:8634091.
10. Lang LA, Kang B, Wang RF, Lang BR. Finite element analysis to determine implant preload. J Prosthet Dent 2003;90:539-46.
11. Morresi AL, D'Amario M, Capogreco M, Gatto R, Marzo G, D'Arcangelo C, Monaco A. Thermal cycling for restorative materials: does a standardized protocol exist in laboratory testing? A literature review. J Mech Behav Biomed Mater 2014;29:295-308.
12. Wittneben JG, Joda T, Weber HP, Brägger U. Screw retained vs. cement retained implant-supported fixed dental prosthesis. Periodontol 2000 2017;73:141-51.
13. Wittneben JG, Millen C, Brägger U. Clinical performance of screw- versus cement-retained fixed implant-supported reconstructions-a systematic review. Int J Oral Maxillofac Implants 2014;29 Suppl:84-98.
14. Savignano R, Soltanzadeh P, Suprono MS. Computational biomechanical analysis of engaging and nonengaging abutments for implant screw-retained fixed dental prostheses. J Prosthodont 2021;30:604-9.
15. Mangano FG, Admakin O, Bonacina M, Lerner H, Rutkunas V, Mangano C. Trueness of 12 intraoral scanners in the full-arch implant impression: a comparative in vitro study. BMC Oral Health 2022;20:263.
16. Rutkunas V, Dirse J, Kules D, Simonaitis T. Misfit simulation on implant prostheses with different combinations of engaging and nonengaging titanium bases. Part 1: stereomicroscopic assessment of the active and passive fit. J Prosthet Dent 2023;129:589-96.
17. Dogus SM, Kurtz KS, Watanabe I, Griggs JA. Effect of engaging abutment position in implant-borne, screw-retained three-unit fixed cantilevered prosthe-

ses. J Prosthodont 2011;20:348-54.
18. Schoenbaum TR, Stevenson RG, Balinghasay E. The hemi-engaging fixed dental implant prosthesis: a technique for improved stability and handling. J Prosthet Dent 2018;120:17-9.
19. Karl M, Winter W, Taylor TD, Heckmann SM. In vitro study on passive fit in implant-supported 5-unit fixed partial dentures. Int J Oral Maxillofac Implants 2004;19:30-7.
20. Brånemark PI. Osseointegration and its experimental background. J Prosthet Dent 1983;50:399-410.
21. Katsoulis J, Takeichi T, Sol Gaviria A, Peter L, Katsoulis K. Misfit of implant prostheses and its impact on clinical outcomes. Definition, assessment and a systematic review of the literature. Eur J Oral Implantol 2017;10 Suppl 1:121-38.
22. Abdelrehim A, Etajuri EA, Sulaiman E, Sofian H, Salleh NM. Magnitude of misfit threshold in implant-supported restorations: a systematic review. J Prosthet Dent 2024;132:528-35.
23. Kano SC, Binon PP, Curtis DA. A classification system to measure the implant-abutment microgap. Int J Oral Maxillofac Implants 2007;22:879-85.
24. Jemt T, Rubenstein JE, Carlsson L, Lang BR. Measuring fit at the implant prosthodontic interface. J Prosthet Dent 1996;75:314-25.
25. Lee H, So JS, Hochstedler JL, Ercoli C. The accuracy of implant impressions: a systematic review. J Prosthet Dent 2008;100:285-91.
26. Wegner K, Weskott K, Zenginel M, Rehmann P, Wöstmann B. Effects of implant system, impression technique, and impression material on accuracy of the working cast. Int J Oral Maxillofac Implants 2013;28:989-95.
27. Abduo J. Fit of CAD/CAM implant frameworks: a comprehensive review. J Oral Implantol 2014;40:758-66.
28. Rutkunas V, Dirse J, Kules D, Mischitz I, Larsson C, Janda M. Misfit simulation on implant prostheses with different combinations of engaging and nonengaging titanium bases. Part 2: screw resistance test. J Prosthet Dent 2024;131:262-71.
29. Alzoubi FM, Sabti M, Alsarraf E, Alshahrani FA, Sadowsky SJ. Evaluation of two implant-supported fixed partial denture abutment designs: Influence on screw surface characteristics. J Prosthodont 2024;33:443-51.
30. Geng JP, Tan KB, Liu GR. Application of finite element analysis in implant dentistry: a review of the literature. J Prosthet Dent 2001;85:585-98.
31. Steiner M, Mitsias ME, Ludwig K, Kern M. In vitro evaluation of a mechanical testing chewing simulator. Dent Mater 2009;25:494-9.
32. Siamos G, Winkler S, Boberick KG. Relationship between implant preload and screw loosening on implant-supported prostheses. J Oral Implantol 2002;28:67-73.
33. Esposito M, Hirsch JM, Lekholm U, Thomsen P. Biological factors contributing to failures of osseointegrated oral implants. Eur J Oral Sci 1998;106:527-51.
34. Zarb GA, Schmitt A. The longitudinal clinical effectiveness of osseointegrated dental implants: the Toronto study. Part III: problems and complications encountered. J Prosthet Dent 1990;64:185-94.
35. Heckmann SM, Karl M, Wichmann MG, Winter W, Graef F, Taylor TD. Loading of bone surrounding implants through three-unit fixed partial denture fixation: a finite-element analysis based on in vitro and in vivo strain measurements. Clin Oral Implants Res 2006;17:345-50.
36. Meijndert CM, Raghoebar GM, Vissink A, Delli K, Meijer HJA. The effect of implant-abutment connections on peri-implant bone levels around single implants in the aesthetic zone: a systematic review and a meta-analysis. Clin Exp Dent Res 2021;7:1025-36.
37. Kim JH, Noh G, Hong SJ, Lee H. Biomechanical stress and microgap analysis of bone-level and tissue-level implant abutment structure according to the five different directions of occlusal loads. J Adv Prosthodont 2020;12:316-21.
38. Sailer I, Mühlemann S, Zwahlen M, Hämmerle CH, Schneider D. Cemented and screw-retained implant reconstructions: a systematic review of the survival and complication rates. Clin Oral Implants Res 2012;23 Suppl 6:163-201.
39. Nissan J, Narobai D, Gross O, Ghelfan O, Chaushu G. Long-term outcome of cemented versus screw-retained implant-supported partial restorations. Int J Oral Maxillofac Implants 2011;26:1102-7.
40. Gaddale R, Mishra SK, Chowdhary R. Complications of screw- and cement-retained implant-supported full-arch restorations: a systematic review and meta-analysis. Int J Oral Implantol (Berl) 2020;13:11-40.